NeuroImage 203 (2019) 116188

Contents lists available at ScienceDirect

NeuroImage

journal homepage: www.elsevier.com/locate/neuroimage

Consistency and dynamical changes of directional information flow in different brain states: A comparison of working memory and resting-state using EEG

Ruimin Wang [a,*], Sheng Ge [b], Noha Mohsen Zommara [c], Karine Ravienna [a], Teodora Espinoza [a], Keiji Iramina [a,d]

[a] Graduate School of Systems Life Sciences, Kyushu University, 744 Motooka Nishi-ku, Fukuoka, Japan
[b] Key Laboratory of Child Development and Learning Science of Ministry of Education, Research Center for Learning Science, School of Biological Science and Medical Engineering, Southeast University, Nanjing, China
[c] Faculty of Design, Department of Human Science, Kyushu University, 4-9-1 Shiobaru Minami-ku, Fukuoka, Japan
[d] Informatics Faculty of Information Science and Electrical Engineering, Kyushu University, 744 Motooka Nishi-ku, Fukuoka, Japan

ARTICLE INFO

Keywords:
Information flow
Phase transfer entropy
Working memory
Resting-state
Alpha oscillations
Theta oscillations

ABSTRACT

Several recent studies have reported a frequency-dependent directional information flow loop in resting-state networks by phase transfer entropy, comprising an anterior-to-posterior information flow in the theta band and a posterior-to-anterior information flow in the alpha band. However, the functional roles of this information flow loop remain unclear. In the current study, we compared information flow patterns in four different brain states using electroencephalography: resting-state, fixation, working memory (WM) encoding and WM maintenance. An auditory (pure tones) WM span task was carried out. A consistent anterior-to-posterior information flow in the theta band and an opposite pattern in the alpha band were found in all four segments. Flows in both patterns were enhanced during WM encoding. In contrast, a prefrontal-to-central information flow in the alpha band was dominant during the resting-state. In addition, enhanced information flows from right temporal to other brain regions in the theta band were found during WM processing (WM encoding and maintenance). Comparison of the consistency and dynamical changes of information flows in these four brain states indicated their functional roles in central executive processes, internal attention, WM information maintenance, and the right-hemisphere advantage in pure tone processing.

1. Introduction

Functional neuroimaging techniques, including functional magnetic resonance imaging (fMRI) and positron emission tomography (PET), are well suited for identifying brain regions exhibiting coincident brain activity, because of their high spatial resolution. However, the data obtained by fMRI (changes in blood oxygenation) and PET (changes in blood flow) provide indirect indices of neural activity, with limited temporal resolution (Dale et al., 2000; Lobier et al., 2014). In contrast, electroencephalography (EEG) and magnetoencephalography (MEG) reveal brain networks directly and have a high temporal resolution (Naghavi and Nyberg, 2005; Sakkalis, 2011).

In EEG and MEG, neural connectivity can be computed from two distinct parameters: amplitude and phase, which analyze neural connectivity from different but complementary perspectives. Amplitude reflects the extent of neural synchrony in a local assembly and sustained activation or deactivation patterns in larger cortical areas (Lobier et al., 2014; Varela et al., 2001). Phase indicates the signal position in a given oscillation cycle and is considered to reflect the coordination of communication across regions in anatomically distributed processing (Lobier et al., 2014). The association between instantaneous EEG phase with particular neuronal firing patterns and neural activity has been reported in previous studies with high temporal precision (Buzsáki and Draguhn, 2004; Harris et al., 2002; Hirase et al., 1999; Sauseng and Klimesch, 2008). Thus, neural connectivity across brain regions is thought to be more accurately reflected by oscillation phase than by amplitude (Cardin et al., 2009; Fries, 2005; Lakatos et al., 2008; Lobier et al., 2014; Ng et al., 2013; Schyns et al., 2011; Singer, 1999;

* Corresponding author.
E-mail address: wang.ruimin.725@s.kyushu-u.ac.jp (R. Wang).

https://doi.org/10.1016/j.neuroimage.2019.116188
Received 15 March 2019; Received in revised form 6 August 2019; Accepted 11 September 2019
Available online 15 September 2019
1053-8119/

Womelsdorf et al., 2007). Moreover, EEG phase synchronization is considered to provide more valuable information about neural connectivity than amplitude estimates (Sauseng and Klimesch, 2008).

In recent years, in order to investigate complex cortical interactions, many researchers have made efforts to improve brain connectivity analysis methods from different, novel perspectives (Frässle et al., 2017; Razi et al., 2017; Sakkalis, 2011; Seguin et al., 2019). Based on EEG phase information, Lobier et al. (2014) proposed a phase-based information flow estimation method called phase transfer entropy (PTE). PTE is a functional connectivity estimation method, which can measure large-scale phase-specific directed connectivity among brain regions using extracted phase time-series data. Lobier et al. (2014) have confirmed that PTE has four advantages for detecting brain connectivity: 1) PTE is reliable even in the combined presence of noise and sensor signal mixing, which can result in reduced connectivity or artificial connectivity; 2) PTE can identify complex interactions; 3) PTE requires limited amounts of data and computation time; 4) PTE is effective for identifying frequency band limited information flow.

Using PTE, Hillebrand et al. (2016) found that the directions of information flow in brain networks during the resting-state are frequency-dependent. In addition, they observed an anterior-to-posterior information flow in the theta band and a posterior-to-anterior information flow pattern in the higher-frequency bands (alpha and beta). These directionally opposite information flows constitute a frequency-specific information flow loop. A consistent information flow pattern in the resting-state has also been reported in other studies using PTE (Dauwan et al., 2016; Engels et al., 2017). The anterior-to-posterior information flow in the theta band reveals that the frontal cortex sends information to all other brain regions in the theta band, reflecting top-down control of the frontal cortex on lower-level, perceptual processes (Hillebrand et al., 2016). According to this top-down control model, Hillebrand et al. (2016) predicted an anterior-to-posterior information flow in the alpha band for attentional control. However, PTE has revealed that the alpha band information flow occurs in a posterior-to-anterior direction. Because information flow was calculated in the resting-state, Hillebrand et al. (2016) proposed two possible explanations: the posterior-to-anterior information flow in the alpha band might reflect internal attention rather than external stimuli; alternatively, the posterior-to-anterior information flow in the alpha band may be a consequence of enhanced top-down signaling in the theta band.

Task-related experiments may be useful for understanding the precise roles of information flow in brain function. In the current study, we examined information flow patterns while participants performed working memory (WM) tasks. WM is the ability to maintain, manipulate, and update information (Chai et al., 2018). A multicomponent WM model was proposed by Baddeley et al., in 2011. In this model, the phonological (maintaining auditory information) and visuo-spatial subsystems (visuospatial information storage) feed into a multidimensional common store (episodic buffer), which interacts with the central executive system. WM networks have been well studied using fMRI, EEG, and MEG. A number of studies using fMRI (Moore et al., 2013; Osaka et al., 2003; Vartanian et al., 2013) and functional near-infrared spectroscopy (fNIRS) (Rodriguez Merzagora et al., 2014) have suggested that a fronto-parietal network underlies WM, and has been suggested to reflect central executive processes. Central executive processes are defined as modality-free supervisory attentional functions with limited capacity, reflecting an interface between the WM and long-term memory systems (Baddeley, 1992; Sauseng et al., 2005). Sauseng et al. (2005) proposed that increased fronto-parietal EEG coherence in the theta band and decreased anterior upper alpha short-range connectivity reflect increased demand on central executive functions in WM. In addition to central executive processes, WM is also related to storage processes, which are thought to involve two subsystems: the phonological loop and the visuospatial sketch (Baddeley, 1992). Brain areas are flexibly connected during different WM modalities. Kawasaki et al. (2014) reported enhanced fronto-temporal and fronto-parietal theta phase synchronization during auditory-verbal and visual WM, respectively. Although central executive functions are thought to be reflected by a frontal-to-parietal information flow in WM processing using theta coupling (Sauseng et al., 2005), no previous studies have comprehensively revealed all possible roles of information flows in WM processing, such as storage, and attentional control. Thus, to explore the precise functional roles of information flows in the current study, we compared the consistency and dynamical changes of information flow in different brain states, including resting-state, fixation, WM encoding, and WM maintenance.

2. Materials and methods

2.1. Participants and recordings

Twenty-one healthy students from Kyushu University (mean age [standard deviation; SD]: 24.28 ± 3.01 years old, range: 19–31; eight females) with intact auditory processing and normal or corrected-to-normal vision participated voluntarily. This study was approved by the ethics committee of Kyushu University. All participants provided written informed consent before the experiment.

EEG data were recorded from 30 active electrodes according to the extended 10–20 system with a sampling rate of 500 Hz using an EEG-amplifier PolymateV AP5148 (TEAC Corp., Tokyo, Japan). The linked earlobes A1 and A2 were used as a reference, and an electrode placed at Fz was used as a ground. For removing eye movement artifacts from EEG data, electrooculography (EOG) signals were simultaneously recorded.

2.2. Experiment design

An auditory span task (as shown in Fig. 1) was carried out. Seven 0.5 s-duration pure tones with frequencies of 338.8, 573.8, 971.9, 1646.2, 2788.4, 4723.1, and 8000 Hz were adopted as stimuli (Cha et al., 2016). Before the experiment, a pre-experiment task was conducted to check that participants could distinguish every sound stimulus. Only participants who were able to distinguish the tones were included in the actual experiment. For all 21 participants, only one participant could not distinguish all the tones correctly. Thus, the analysis was conducted using the data from only 20 participants.

During the encoding period, a series of pure tones with an interval of 0.8 s were presented via earphones. Five different workload auditory span tasks (three to seven pure tones) were conducted randomly, without any instruction about how many sounds the participant would hear. After

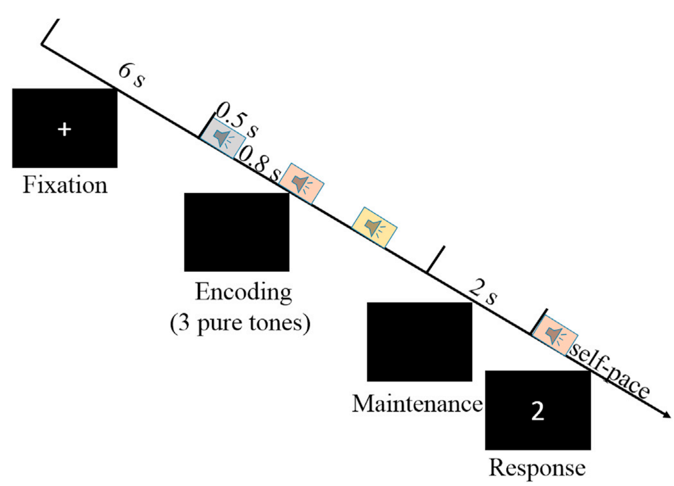

Fig. 1. Experiment protocol: an example trial for three auditory span task. During the experiment, five different workload auditory span tasks (three to seven pure tones) were presented randomly. Participants received no instructions regarding how many sounds would be presented in a given trial.

a 2 s maintenance period, a probe tone was played. Participants were asked to report the order position of the probe tone using a keyboard. In total, 80 trials (sixteen trials for each workload) were completed by each participant. After finishing the WM task, participants were asked to close their eyes for 2 min to record resting-state EEG data.

2.3. EEG data pre-processing

EOG artifacts were removed from EEG data using independent component analysis (ICA). A 60 Hz notch filter and a bandpass filter (0.1–110 Hz) were applied to remove electrical interference and other artifacts. EEG data were then resampled at 250 Hz.

Artifact-free EEG data were further segmented into four different types of epochs: 1) 2 min eyes-closed resting-state; 2) 2 s fixation before memory encoding; 3) memory encoding state with 3.9 s, 5.2 s, 6.5 s, 7.8 s, and 9.1 s durations for each workload condition, respectively; and 4) 2 s WM maintenance.

2.4. Individual EEG frequency bands

According to the typical EEG/MEG power density spectrum described by Moretti et al. (2004), we calculated each participant's specific frequency bands using 2-min eyes-closed resting-state EEG data. The averaged frequency ranges ($mean \pm SD$) for each band were: delta, $2-2.82\pm 0.12Hz$; theta, $3.83\pm0.12-6.17\pm0.18Hz$; alpha, $7.22\pm0.18-12.24\pm 0.16Hz$; beta, $14.32\pm0.12-29Hz$; and gamma1, $30-59Hz$.

2.5. Phase transfer entropy

Transfer entropy (TE) is based on the following principle: if a source signal X has a causal influence on a target signal Y, the uncertainty of the present of $Y(t)$ conditioned on its own past $Y(t-\delta)$ should be greater than the uncertainty of the present of $Y(t)$ conditioned on the signals of both past $X(t-\delta)$ and $Y(t-\delta)$. The uncertainty of a variable signal X is quantified by Shannon Entropy $H(X) = -\sum_x p(x)\log p(x)$. Thus, TE can be represented by the following equation (Lobier et al., 2014):

$$TE_{X\to Y} = H(Y(t)|Y(t-\delta)) - H(Y(t)|Y(t-\delta), X(t-\delta)) \quad (1)$$

Using a Morlet wavelet or Hilbert transform, a time-series of the signal $X(t)$ in a given frequency band can be represented in a complex form $X(t) = A(t)\exp(i\theta(t))$, where $A(t)$ is the instantaneous amplitude and $\theta(t)$ is the instantaneous phase time-series. Based on the TE model, a phase-specific directed connectivity estimation method, PTE, was proposed by Lobier et al. (2014), represented by the following equation:

$$\begin{aligned} PTE_{X\to Y} = {} & H\big(\theta_y(t), \theta_y(t-\delta)\big) + H\big(\theta_y(t-\delta), \theta_x(t-\delta)\big) \\ & -H\big(\theta_y(t-\delta)\big) - H\big(\theta_y(t), \theta_y(t-\delta), \theta_x(t-\delta)\big) \end{aligned} \quad (2)$$

To reduce bias, Hillebrand et al. (2016) proposed the following normalization equation:

$$dPTE_{X\to Y} = PTE_{X\to Y}/(PTE_{X\to Y} + PTE_{Y\to X}) \quad (3)$$

The value range of $dPTE_{X\to Y}$ is between 0 and 1. Whereas $0.5 < dPTE_{X\to Y} \le 1$ indicates preferential information flow from X to Y, $0 \le dPTE_{X\to Y} < 0.5$ indicates preferential information flow from Y to X, and $dPTE_{X\to Y} = 0.5$ indicates there is no directed information flow.

The values of $dPTE_{X\to Y}$ were further subtracted by 0.5. Thus, Positive values indicate that information flowed preferentially from X to Y. In contrast, negative values indicate that information flowed preferentially toward X from Y. A value of zero indicates that there was no directed information flow between electrodes.

We first evaluated the $dPTE_{X\to Y}$ values of all possible electrode-pairs from the 30-channel EEG data of each trial, resulting in a 30×30 matrix. Second, the 30 electrodes were divided into seven regions of interest (ROIs): prefrontal (AFz, AF7, AF8, F3, F4, F7, F8), agranular frontal (FC3, FCz, FC4, C3, Cz, and C4), left temporal (T7, and FT7), right temporal (T8, and FT8), preparietal (CP1, CP2, CP5, and CP6), parietal (P3, Pz, and P4), and occipital cortex (P7, P8, POz, O1, Oz, and O2). The information flow strength between two ROIs (e.g., prefrontal cortex vs occipital cortex) was calculated as the following equation:

$$dPTE_{prefrontal\to occipital} = \frac{1}{MN}\sum_{m=1}^{M}\sum_{n=1}^{N} dPTE_{X(m)\to Y(n)} \quad (4)$$

where X is the electrodes in the prefrontal cortex, Y is electrodes in the occipital cortex, M is the number of electrodes in X, and N is the number of electrodes in Y. The information strengths between all possible ROI pairs were calculated, resulting in a 7×7 matrix.

For each participant, the dPTE between ROIs (7×7) were averaged across all the trials of the same brain state, resulting in a $7\times 7\times 4$ matrix. Here, number 4 refers to four brain states, resting, fixation, WM encoding, and WM maintenance. Because the PTE values of WM encoding (and maintenance) between different workloads showed no significant differences, the PTE values of WM encoding (and WM maintenance) were averaged from all five workload tasks. Thus, the information flows between ROIs in fixation, WM encoding, and WM maintenance were averaged from 80 trials for each participant. For the 2-min-eyes-closed resting-state, there was only one trial for a participant.

Finally, participant-averaged information flow strengths ($mean \pm SE$ [standard error]) between ROIs across all 20 participants were calculated for each brain state. SE refers to the individual standard error.

All data processing was achieved using the BrainStorm software package (http://neuroimage.usc.edu/brainstorm).

2.6. Statistics analysis

According to the Lilliefors test, not all PTE values followed a normal distribution. Thus, a non-parametric statistic, permutation test, was applied in this study. Permutation test has been adopted for testing the significance of PTE information flows in previous studies (Hillebrand et al., 2016; Lobier et al., 2014).

First, to confirm whether the information flows between two ROIs under the four brain states were significantly directed or not, a dataset (20×4, each row corresponds to a particular participant while each column represents a brain state) consisted of information flow strengths in the four states of 20 individuals was used for the permutation test. 5000 random permutations were implemented to check whether the information flow strengths were significantly different from zero or not. The null distributions are symmetrically generated around the mean of the null hypothesis. A p-value was obtained for each brain state, which was adjusted by "tmax" method for multiple comparisons to control family-wise error (Blair and Karnisky, 1993; Westfall and Young, 1993). The permutation tests were conducted using a widely used Matlab function "mult_comp_perm_t1", developed by Groppe et al., in 2011 (version 1.8, https://jp.mathworks.com/matlabcentral/fileexchange/29782-mult_comp_perm_t1). The validity of this function has been confirmed in many EEG studies (Barrick and Dillon, 2018; Files et al., 2016; Mehnert et al., 2019).

Second, Friedman's test followed by a multiple comparisons post hoc test with Tukey-Kramer correction was used to test if there was a significant difference between different brain states (resting-state, fixation, WM encoding, and WM maintenance).

3. Results

EEG data recorded from 20 participants who performed an auditory span task were segmented into four brain states: eyes-closed resting-state, fixation, WM encoding, and WM maintenance. Information flow loops were observed for all four phase segments, consistent with previous reports (Dauwan et al., 2016; Engels et al., 2017; Hillebrand et al., 2016), exhibiting an anterior-to-posterior flow in the theta band (see Fig. 2) and a posterior-to-anterior information flow in the alpha band (see Fig. 3).

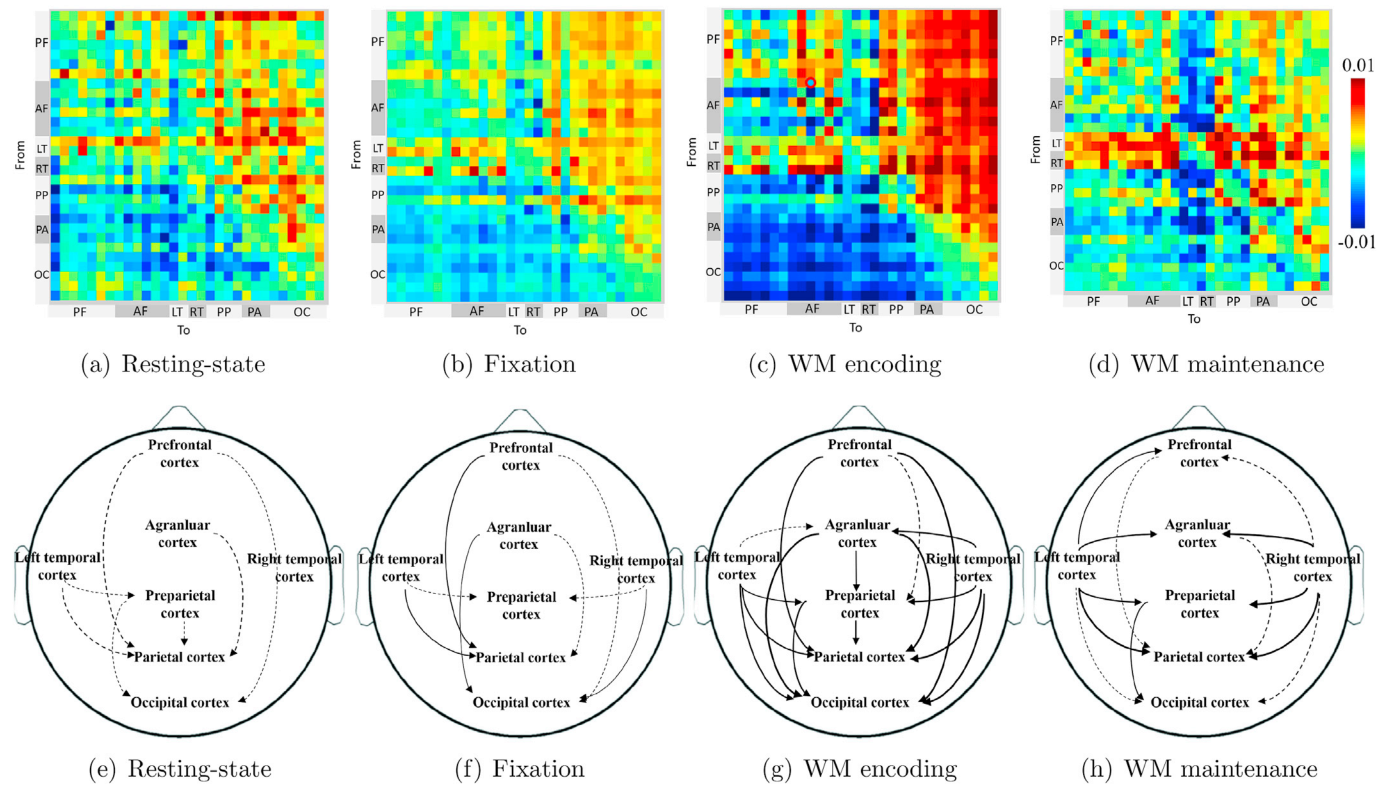

Fig. 2. Averaged PTE matrices from all participants in the theta band for four different phase segments: (a) 2-min-eyes-closed resting-state, (b) 2-s fixation in front of WM, (c) WM encoding, and (d) 2-s WM maintenance. Each color square in the PTE matrices represents information strength between an electrode pair. (e)–(h) are information flows among the brain regions. The solid lines indicate significant directional information flows between regions (permutation test, $p < 0.05$). Line thickness represents information flow strength (greater thicknesses indicate higher values). The minimum strength of all the significant directional information flows among the four brain states is 0.003. We set 0.003 as a threshold. Information flows over the threshold without significantly directed (permutation test, $p > 0.05$) were plotted in dashed lines (see Supplementary Fig. S1 for details). PF: prefrontal; AF: agranular frontal; LT: left temporal; RT: right temporal; PP: preparietal; PA: parietal; OC: occipital.

The information flows in the other bands (delta, beta, and gamma1) were dispersed and weak.

For WM encoding state, both of the information flows from the frontal to parietal-occipital cortex in the theta band and parietal-to-frontal in the alpha band were enhanced compared with the other three states. 1) The information flow strengths of theta band ($mean \pm SE$) from frontal (prefrontal, and agranular frontal) to parietal-occipital cortex in the four EEG segments were (see Fig. 4 (a)): resting-state, 0.003 ± 0.002 (permutation test, $p = 0.121$); fixation, 0.003 ± 0.001 (permutation test, $p = 0.036$); encoding, 0.007 ± 0.002 (permutation test, $p = 0.002$); and maintenance, 0.003 ± 0.002 (permutation test, $p = 0.281$). According to the permutation test, only fixation and WM encoding states exhibited directed information flow from the frontal to parietal-occipital cortex in the theta band. Friedman's test with Tukey-Kramer correction indicated that this information flow in the WM encoding state was significantly stronger than in fixation ($p = 0.025$) and WM maintenance states ($p = 0.008$). However, there was no significant difference between encoding and resting-state ($p = 0.092$). 2) The information flow strengths ($mean \pm SE$) for parietal-to-frontal in the alpha band were (see Fig. 4 (e)): resting-state, 0 ± 0.007 (permutation test, $p = 0.500$); fixation, 0.007 ± 0.004 (permutation test, $p = 0.144$); encoding, 0.020 ± 0.006 (permutation test, $p = 0.004$); and maintenance, 0.005 ± 0.005 (permutation test, $p = 0.284$). Only WM encoding showed directed information flow from the parietal-to-frontal cortex in the alpha band. The parietal-to-frontal information flow in encoding was significantly stronger than that in resting-state (Friedman's test, $p = 0.002$), fixation (Friedman's test, $p = 0.049$), and maintenance (Friedman's test, $p = 0.036$). The fronto-parietal network has been suggested to reflect the central executive functions of WM by fMRI (Moore et al., 2013; Osaka et al., 2003; Vartanian et al., 2013), fNIRS (Rodriguez Merzagora et al., 2014), and EEG (Sauseng et al., 2005).

Different from information flows from the parietal-to-frontal cortex in the alpha band, the information flows from the occipital-to-frontal cortex (prefrontal cortex, and agranular frontal cortex) were consistently directed for all four segments without any significant differences (see Fig. 4 (f)). The information flow strengths ($mean \pm SE$) for occipital-to-frontal in the four segments were: resting-state, 0.021 ± 0.006 (permutation test, $p = 0.002$); fixation, 0.018 ± 0.003 (permutation test, $p = 0$); encoding, 0.026 ± 0.006 (permutation test, $p = 0.0003$); and maintenance, 0.019 ± 0.004 (permutation test, $p = 0.0002$).

In the alpha band, in addition to the posterior-to-anterior information flows, information flows from the prefrontal region to central regions (agranular frontal, temporal, and preparietal regions) were also observed for the resting-state (see Fig. 4 (d)). The information flow strength ($mean \pm SE$) of prefrontal-to-central for the four segments were: resting-state, 0.024 ± 0.005 (permutation test, $p = 0.0001$); fixation, 0.005 ± 0.003 (permutation test, $p = 0.097$); encoding, 0.003 ± 0.003 (permutation test, $p = 0.311$); and maintenance, 0.006 ± 0.003 (permutation test, $p = 0.082$). Friedman's test indicated that this flow strength in the resting-state was significantly stronger than the other three EEG segments, $p = 0.017$ compared with fixation, $p = 0.036$ compared with encoding, and $p = 0.008$ compared with maintenance.

Kawasaki et al. (2014) reported that brain areas are flexibly connected during different WM modalities: fronto-temporal and fronto-parietal theta phase synchronization are enhanced during auditory-verbal and visual WM, respectively. However, in our study, directed information flows in the theta band from the temporal cortex, particularly from the right temporal cortex, to both the agranular frontal

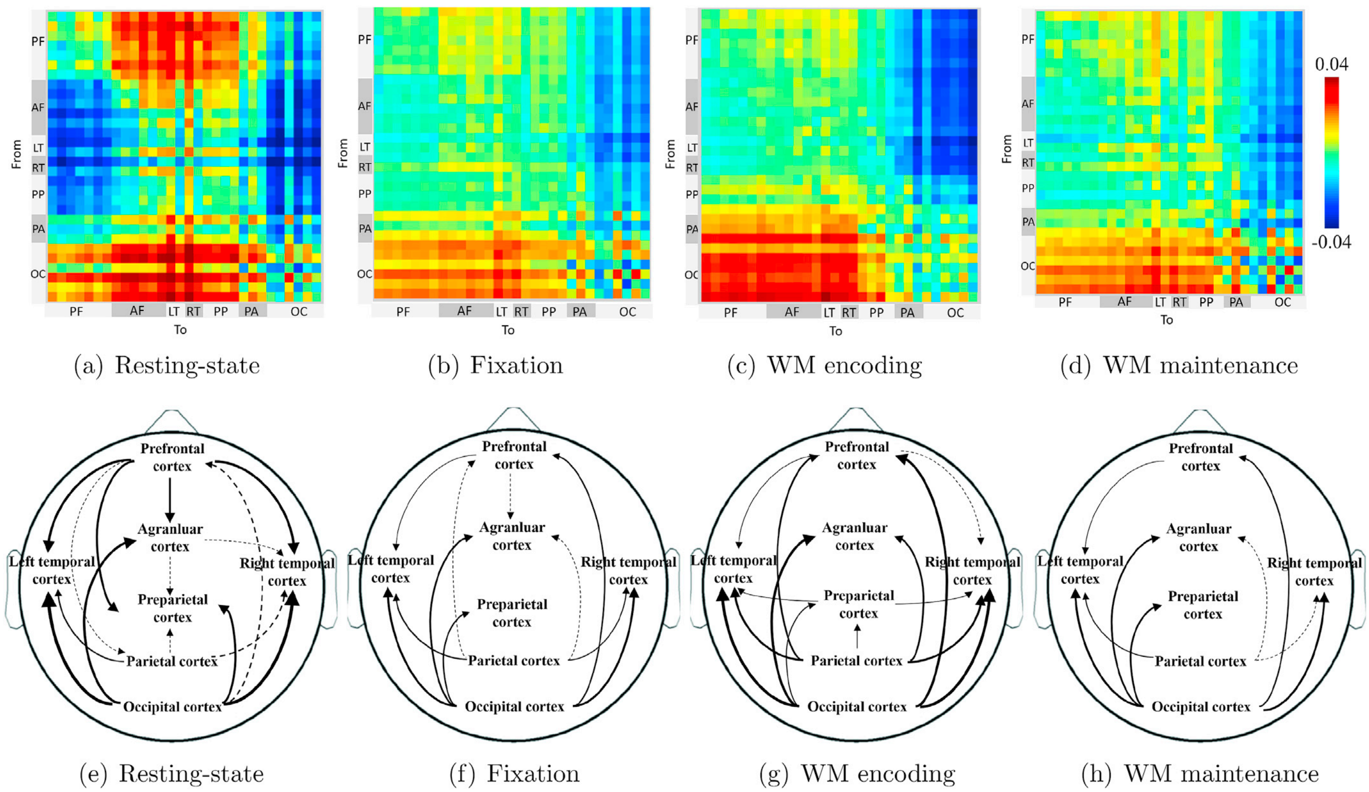

Fig. 3. Averaged PTE matrices from all participants in the alpha band for four different phase segments: (a) 2-min-eyes-closed resting-state, (b) 2-s fixation in front of WM, (c) WM encoding, and (d) 2-s WM maintenance. Each color square in the PTE matrices represents information strength between an electrode pair. (e)–(h) are information flows among the brain regions. The solid lines indicate significant directional information flows between regions (permutation test, $p < 0.05$). Line thickness represents information flow strength (greater thicknesses indicate higher values). The minimum strength of all the significant directional information flows among the four brain states is 0.006. We set 0.006 as a threshold. Information flows over the threshold without significantly directed (permutation test, $p > 0.05$) were plotted in dashed lines (see Supplementary Fig. S1 for details). PF: prefrontal; AF: agranular frontal; LT: left temporal; RT: right temporal; PP: preparietal; PA: parietal; OC: occipital.

and parietal-occipital cortex, were significantly involved in WM encoding and maintenance states (see Fig. 2). 1) The information flow strengths (*mean* $\pm$ *SE*) from right temporal to agranular frontal cortex and preparietal regions in the four EEG segments were (see Fig. 4 (b)): resting-state, -0.001 ± 0.002 (permutation test, $p = 0.493$); fixation, 0.002 ± 0.001 (permutation test, $p = 0.133$); encoding, 0.006 ± 0.002 (permutation test, $p = 0.008$); and maintenance, 0.007 ± 0.002 (permutation test, $p = 0.001$). The information flow strengths in encoding and maintenance were significantly higher than that in the resting-state (Friedman's test, $p = 0.008$ for encoding and $p = 0.035$ for maintenance, compared with resting-state respectively). There were no significant differences between encoding (Friedman's test, $p = 0.316$) or maintenance (Friedman's test, $p = 0.611$) with fixation. 2) The information flow strengths (*mean* $\pm$ *SE*) from right temporal to parietal-occipital cortex in the four EEG segments were (see Fig. 4 (c)): resting-state, 0.002 ± 0.002 (permutation test, $p = 0.404$); fixation, 0.003 ± 0.001 (permutation test, $p = 0.064$); encoding, 0.007 ± 0.002 (permutation test, $p = 0.0004$); and maintenance, 0.005 ± 0.002 (permutation test, $p = 0.027$). The information flow strength in encoding was significantly higher than that in resting-state (Friedman's test, $p = 0.025$) and fixation (Friedman's test, $p = 0.025$), respectively. There was no significant difference between maintenance and other brain states.

WM encoding and maintenance also involved significant directed information flow from the left temporal to other regions. The information flows from the left temporal cortex and from the right temporal cortex showed no significant differences. However, for the information flows from the left temporal cortex, there were no significant differences between different brain states. 1)The information flow strengths (*mean* $\pm$ *SE*) from left temporal to agranular frontal cortex and preparietal regions in the four EEG segments were: resting-state, 0.003 ± 0.002 (permutation test, $p = 0.151$); fixation, 0.003 ± 0.002 (permutation test, $p = 0.116$); encoding, 0.004 ± 0.002 (permutation test, $p = 0.049$); and maintenance, 0.006 ± 0.002 (permutation test, $p = 0.022$). 2) The information flow strengths (*mean* $\pm$ *SE*) from the left temporal to parietal-occipital cortex in the four EEG segments were: resting-state, 0.003 ± 0.002 (permutation test, $p = 0.119$); fixation, 0.003 ± 0.001 (permutation test, $p = 0.049$); encoding, 0.006 ± 0.001 (permutation test, $p = 0.002$); and maintenance, 0.004 ± 0.002 (permutation test, $p = 0.047$).

4. Discussion

4.1. Information flow loop

Long-range functional interaction or integration between distinct cortical areas are achieved by slow oscillations in theta and alpha band activities (Min and Park, 2010; Sauseng et al., 2005). Information flow loop, composed of anterior-to-posterior information flow in the theta band and an opposite pattern in the alpha band, has been reported in the resting-state (Dauwan et al., 2016; Engels et al., 2017; Hillebrand et al., 2016). In addition to the resting-state, we also observed this information flow loop during fixation, WM encoding, and WM maintenance. Although the information flow patterns in different brain states were consistent to some extent, significant differences (i.e., information flow strength, sub-networks) among these brain states were found in the current study. For example, information flows from prefrontal to central cortex in the alpha band were only observed in the resting-state. These dynamical changes in theta/alpha information flow strengths in sub-networks according to brain states may help to elucidate their

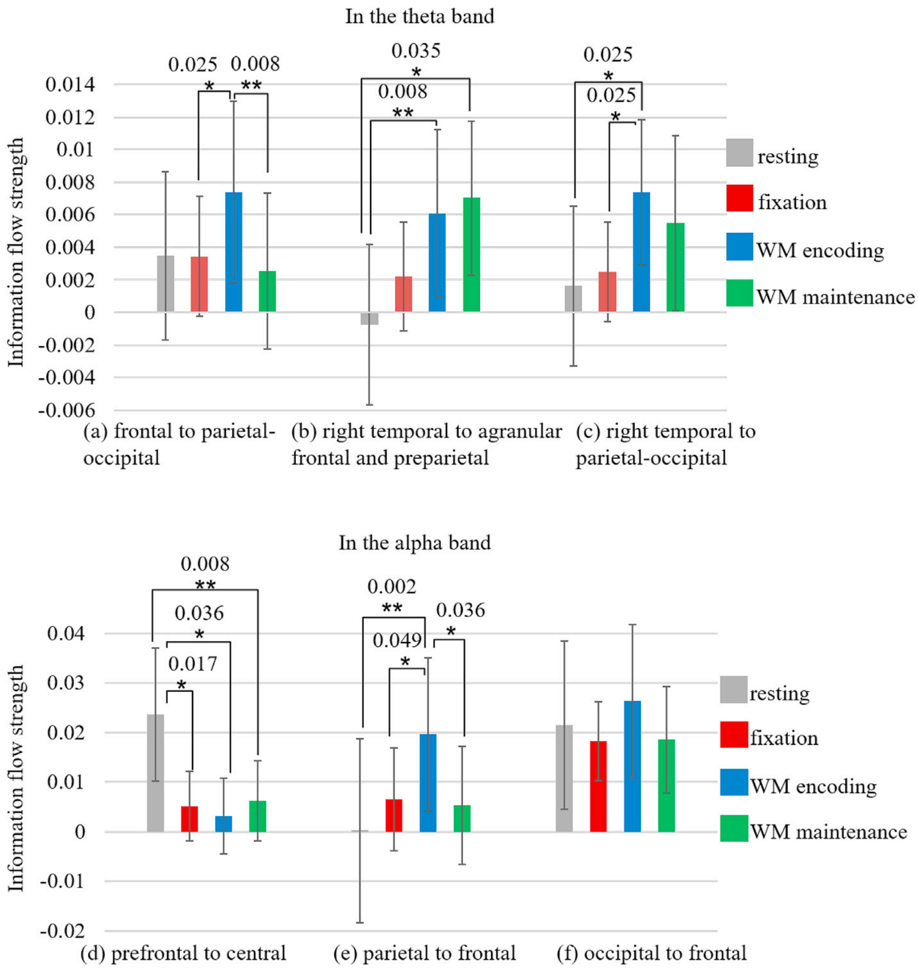

Fig. 4. Information flow strengths in the four brain states: (a)–(c) in the theta band, (d)–(f) in the alpha band. * represents $p < 0.05$, and ** represents $p < 0.01$. Error bars indicate 95% confidence intervals (CIs) of the averaged information flow strengths of all participants. CIs were calculated using a Matlab function "tmaxPermCIsOneSamp", developed by Groppe in 2017 (version 1.0, https://jp.mathworks.com/matlabcentral/fileexchange/54573-tmaxpermcisonesamp). This function computes symmetric multiple comparison adjusted CIs by permuting the residuals of a data set. 5000 random permutations were computed.

functional roles in neural processing.

4.2. Enhanced fronto-parietal networks reflect central executive functions of WM

A fronto-parietal network, composed of the dorsolateral prefrontal cortex (DLPFC), the anterior cingulate cortex (ACC), and the parietal cortex (PAR) have been suggested to comprise the WM neural network (Moore et al., 2013; Osaka et al., 2003; Rodriguez Merzagora et al., 2014; Vartanian et al., 2013). The DLPFC is involved in executive control, the ACC is regarded as an "attention controller", and the PAR is considered to control sensory or perceptual processing (Baddeley, 2010; Chai et al., 2018). In addition to its role in WM, the fronto-parietal network is reported to be commonly activated during conscious perception, attention, and episodic retrieval, and has been suggested to reflect central executive control processes (Babiloni et al., 2004; Kondo et al., 2004; Li et al., 2004; Osaka et al., 2004). Functionally, the prefrontal cortex is suggested to be involved in actively focusing attention on relevant sensory representations, selecting information and performing executive functions that are necessary for controlling the cognitive processing of information (Gerrits et al., 2015; Lara and Wallis, 2015; Postle, 2006).

By comparing the information flow strengths in the four EEG segments, an enhanced information flow from frontal to parietal-occipital in the theta band, and a reversed enhanced parietal-to-frontal information flow in the alpha band were observed in the WM encoding state. This finding supports the notion that an increase in theta/alpha long-range coherence reflects increased demands on central executive functions in working memory (Sauseng et al., 2005).

4.3. Prefrontal-to-central information flows in the alpha band reflect internal attention

There are at least two distinct subsystems in the default mode network (DMN): a memory process system and a self-relevant mental system. An fMRI study by Gusnard et al. (2001) revealed that the medial prefrontal cortex (MPFC) was more active during self-referential tasks compared with attention-demanding tasks. The MPFC plays a role in evaluation and judgment of self-referential stimuli (Yaoi et al., 2015). Forbes et al. (2015) reported that the lateral parietal cortex (LPC) and MPFC were phase-locked in the alpha band during self-concept processing, confirming that phase-locking in the alpha band was related to self-referential stimuli. Similarly, we found enhanced prefrontal-to-central (agranular frontal, temporal, and preparietal) information flow in the alpha band only for the resting-state. Thus, the prefrontal-to-central information flow in the alpha band might reflect internal attention rather than external stimuli.

4.4. Occipital-to-frontal information flows reflect baseline brain connectivity

Posterior-to-anterior information flows in the alpha band have been reported in previous studies during the resting-state (Dauwan et al., 2016; Engels et al., 2017; Hillebrand et al., 2016). In the current study, we found that the parietal-to-frontal information flows in WM encoding were significantly stronger than in the other three brain states. However, the occipital-to-frontal information flows in the alpha band were consistently strong in all four brain states. We further compared the occipital-to-frontal information flow strengths with the parietal-to-frontal information flow strengths. All four brain states were found to show significant differences using permutation tests: resting-state, $p = 0.0001$; fixation, $p = 0.0001$; encoding, $p = 0.037$; and maintenance, $p = 0.0003$. Thus, the occipital-to-frontal and parietal-to-frontal information flows were two distinct networks.

As discussed previously, the parietal-to-frontal information flows in the alpha band in the WM encoding reflect increased demand on central executive functions in WM (see section 4.2 "Enhanced fronto-parietal networks reflect central executive functions of WM"). However, the functional roles of occipital-to-frontal information flows are difficult to explain in accord with our current experimental results. Decreased occipital-to-frontal correlation during drowsiness-alpha activity was reported by Cantero et al. (2002). Thul et al. (2016) reported reduced feedback interaction in fronto-occipital networks in patients with unresponsive-wakefulness-syndrome. In the current study, participants were instructed to remain alert during the whole experiment. The occipital-to-frontal information flow pattern in the alpha band may indicate arousal, or other baseline brain activity. Further research is needed to confirm the functional roles of occipital-to-frontal information flows.

4.5. Theta oscillations in WM information maintenance

In the current study, we observed enhanced information flows from right temporal to agranular frontal and parietal during both WM encoding and maintenance. The connections among frontal, temporal, and parietal regions have been reported using theta phase synchronization: frontal-temporal theta synchronization has been reported during WM encoding, maintenance, and retrieval processes (Kawasaki et al., 2014; Sarnthein et al., 1998; Sauseng et al., 2004; Serrien et al., 2004); fronto-parietal theta synchronization is reported to be enhanced when processing high workload and complex manipulation (Kopp et al., 2006; Payne and Kounios, 2009; Sauseng et al., 2005). However, Kawasaki et al. (2014) reported that fronto-temporal synchronization was involved in auditory-verbal WM tasks and that fronto-parietal synchronization was involved in visual WM tasks. We inferred that auditory WM tasks not only induce temporal-to-agranular frontal but also temporal-to-parietal information flows. Thus, we concluded that the information flow from right temporal to agranular frontal and parietal reflects the functional role of theta activity in the transient maintenance of information in WM rather than top-down control. Several other studies also support the functional roles of theta activity in transient maintenance of information in WM using theta coherence (Sarnthein et al., 1998; Sauseng et al., 2004; Sauseng et al., 2006; Weiss et al., 2000).

Both of the information flows from the left temporal cortex and right temporal cortex were significantly directed in WM processing, and with no significant differences between them. However, information flow strengths from the left temporal cortex in WM processing did not show significant differences with resting or fixation states. This possibly because of a right-hemisphere advantage in pure tone processing. Pure tones were used as WM stimuli in the current study. The right-hemisphere advantage in pure tone processing has been confirmed in many previous studies (Hine and Debener, 2007; Koike et al., 1996; Lütkenhöner et al., 2003; Sidtis, 1984). Koike et al. (1996) found that patients with the right temporal cortex removed were found to exhibit impaired performance on pure tone timbre discrimination and tonal memory tasks. However, this phenomenon was not observed in patients with the left temporal cortex removed. In a recent study, Matsubara et al. (2018) conducted a pure tone stimulation test in patients with mesial temporal cortex epilepsy (mTLE). Patients with right mTLE exhibited more pronounced abnormalities in auditory cortex function than patients with left mTLE and healthy controls. Responses was predominantly observed in the right hemisphere in both left mTLE patients and healthy controls.

5. Conclusion

In the current study, we compared the information flow patterns of four EEG segments: resting-state, fixation, WM encoding and WM maintenance. Dominant anterior-to-posterior information flow in the theta band and an opposite pattern in the alpha band were found in all four segments. By comparing the consistency and dynamical changes of the information flow in different brain states, various brain functions were found to be related to information flow in the current study, including internal attention, central executive functions, WM information maintenance, and the right-hemisphere advantage in pure tone processing. Thus, the current results further confirmed that information flow can be useful for understanding neural correlations, and that PTE provides a robust approach for evaluating information flow.

Conflicts of interest

The authors declare no conflict of interest.

Data and code availability statement

The data that support the findings of this study are available from the corresponding author upon reasonable request.

Appendix A. Supplementary data

Supplementary data to this article can be found online at https://doi.org/10.1016/j.neuroimage.2019.116188.

References

Babiloni, C., Babiloni, F., Carducci, F., Cappa, S.F., Cincotti, F., Del Percio, C., Miniussi, C., Moretti, D.V., Rossi, S., Sosta, K., Rossini, P.M., 2004. Human cortical rhythms during visual delayed choice reaction time tasks: A high-resolution EEG study on normal aging. Behav. Brain Res. 153, 261–271. https://doi.org/10.1016/j.bbr.2003.12.012.

Baddeley, A., 1992. Working memory. Science 255, 556–559. https://doi.org/10.1126/science.1736359.

Baddeley, A., 2010. Working memory. Curr. Biol. 20, R136–R140. https://doi.org/10.1016/j.cub.2009.12.014.

Baddeley, A.D., Allen, R.J., Hitch, G.J., 2011. Binding in visual working memory: The role of the episodic buffer. Neuropsychologia 49, 1393–1400. https://doi.org/10.1016/j.neuropsychologia.2010.12.042.

Barrick, E.M., Dillon, D.G., 2018. An ERP study of multidimensional source retrieval in depression. Biol. Psychol. 132, 176–191. https://doi.org/10.1016/j.biopsycho.2018.01.001.

Blair, R.C., Karniski, W., 1993. An alternative method for significance testing of waveform difference potentials. Psychophysiology 30, 518–524. https://doi.org/10.1111/j.1469-8986.1993.tb02075.x.

Buzsáki, G., Draguhn, A., 2004. Neuronal oscillations in cortical networks. Science 304, 1926–1929. https://doi.org/10.1126/science.1099745.

Cantero, J.L., Atienza, M., Salas, R.M., 2002. Human alpha oscillations in wakefulness, drowsiness period, and REM sleep: different electroencephalographic phenomena within the alpha band. Neurophysiol. Clin. 32, 54–71. https://doi.org/10.1016/S0987-7053(01)00289-1.

Cardin, J.A., Carlén, M., Meletis, K., Knoblich, U., Zhang, F., Deisseroth, K., Tsai, L.-H., Moore, C.I., 2009. Driving fast-spiking cells induces gamma rhythm and controls sensory responses. Nature 459, 663–667. https://doi.org/10.1038/nature08002.

Cha, K., Zatorre, R.J., Schönwiesner, M., 2016. Frequency selectivity of voxel-by-voxel functional connectivity in human auditory cortex. Cerebr. Cortex 26, 211–224. https://doi.org/10.1093/cercor/bhu193.

Chai, W.J., Abd Hamid, A.I., Abdullah, J.M., 2018. Working memory from the psychological and neurosciences perspectives: a review. Front. Psychol. 9, 401. https://doi.org/10.3389/fpsyg.2018.00401.

Dale, A.M., Liu, A.K., Fischl, B.R., Buckner, R.L., Belliveau, J.W., Lewine, J.D., Halgren, E., 2000. Dynamic statistical parametric mapping: combining fMRI and MEG for high-resolution imaging of cortical activity. Neuron 26, 55–67. https://doi.org/10.1016/S0896-6273(00)81138-1.

Dauwan, M., van Dellen, E., van Boxtel, L., van Straaten, E.C.W., de Waal, H., Lemstra, A.W., Gouw, A.A., van der Flier, W.M., Scheltens, P., Sommer, I.E., Stam, C.J., 2016. EEG-directed connectivity from posterior brain regions is decreased in dementia with Lewy bodies: a comparison with Alzheimer's disease and controls. Neurobiol. Aging 41, 122–129. https://doi.org/10.1016/j.neurobiolaging.2016.02.017.

Engels, M.M.A., Yu, M., Stam, C.J., Gouw, A.A., van der Flier, W.M., Scheltens, P., van Straaten, E.C.W., Hillebrand, A., 2017. Directional information flow in patients with Alzheimer's disease. A source-space resting-state MEG study. Neuroimage. Clin. 15, 673–681. https://doi.org/10.1016/j.nicl.2017.06.025.

Files, B.T., Lawhern, V.J., Ries, A.J., Marathe, A.R., 2016. A permutation test for unbalanced paired comparisons of global field power. Brain Topogr. 29, 345–357. https://doi.org/10.1007/s10548-016-0477-3.

Forbes, C.E., Leitner, J.B., Duran-Jordan, K., Magerman, A.B., Schmader, T., Allen, J.J., 2015. Spontaneous default mode network phase-locking moderates performance perceptions under stereotype threat. Soc. Cogn. Affect. Neurosci. 10, 994–1002. https://doi.org/10.1093/scan/nsu145.

Frässle, S., Lomakina, E.I., Razi, A., Friston, K.J., Buhmann, J.M., Stephan, K.E., 2017. Regression DCM for fMRI. Neuroimage 155, 406–421. https://doi.org/10.1016/j.neuroimage.2017.02.090.

Fries, P., 2005. A mechanism for cognitive dynamics: neuronal communication through neuronal coherence. Trends Cogn. Sci. 9, 474–480. https://doi.org/10.1016/j.tics.2005.08.011.

Gerrits, N.J., van der Werf, Y.D., Verhoef, K.M., Veltman, D.J., Groenewegen, H.J., Berendse, H.W., van den Heuvel, O.A., 2015. Compensatory fronto-parietal hyperactivation during set-shifting in unmedicated patients with Parkinson's disease. Neuropsychologia 68, 107–116. https://doi.org/10.1016/j.neuropsychologia.2014.12.022.

Groppe, D.M., Urbach, T.P., Kutas, M., 2011. Mass univariate analysis of event-related brain potentials/fields I: A critical tutorial review. Psychophysiology 48, 1711–1725. https://doi.org/10.1111/j.1469-8986.2011.01273.x.

Groppe, D.M., 2017. Combating the scientific decline effect with confidence (intervals). Psychophysiology 54, 139–145. https://doi.org/10.1111/psyp.12616.

Gusnard, D.A., Akbudak, E., Shulman, G.L., Raichle, M.E., 2001. Medial prefrontal cortex and self-referential mental activity: Relation to a default mode of brain function. Proc. Natl. Acad. Sci. U. S. A 98, 4259–4264. https://doi.org/10.1073/pnas.071043098.

Harris, K.D., Henze, D.A., Hirase, H., Leinekugel, X., Dragoi, G., Czurkó, A., Buzsáki, G., 2002. Spike train dynamics predicts theta-related phase precession in hippocampal pyramidal cells. Nature 417, 738–741. https://doi.org/10.1038/nature00808.

Hillebrand, A., Tewarie, P., van Dellen, E., Yu, M., Carbo, E.W.S., Douw, L., Gouw, A.A., van Straaten, E.C., Stam, C.J., 2016. Direction of information flow in large-scale resting-state networks is frequency-dependent. Proc. Natl. Acad. Sci. U. S. A 113, 3867–3872. https://doi.org/10.1073/pnas.1515657113.

Hine, J., Debener, S., 2007. Late auditory evoked potentials asymmetry revisited. Clin. Neurophysiol. 118, 1274–1285. https://doi.org/10.1016/j.clinph.2007.03.012.

Hirase, H., Czurkó, A., Csicsvari, J., Buzsáki, G., 1999. Firing rate and theta-phase coding by hippocampal pyramidal neurons during 'space clamping'. Eur. J. Neurosci. 11, 4373–4380. https://doi.org/10.1046/j.1460-9568.1999.00853.x.

Kawasaki, M., Kitajo, K., Yamaguchi, Y., 2014. Fronto-parietal and fronto-temporal theta phase synchronization for visual and auditory-verbal working memory. Front. Psychol. 5 (200). https://doi.org/10.3389/fpsyg.2014.00200.

Koike, A., Shimizu, H., Suzuki, I., Ishijima, B., Sugishita, M., 1996. Preserved musical abilities following right temporal lobectomy. J. Neurosurg. 85, 1000–1004. https://doi.org/10.3171/jns.1996.85.6.1000.

Kondo, H., Morishita, M., Osaka, N., Osaka, M., Fukuyama, H., Shibasaki, H., 2004. Functional roles of the cingulo-frontal network in performance on working memory. Neuroimage 21, 2–14. https://doi.org/10.1016/j.neuroimage.2003.09.046.

Kopp, F., Schröger, E., Lipka, S., 2006. Synchronized brain activity during rehearsal and short-term memory disruption by irrelevant speech is affected by recall mode. Int. J. Psychophysiol. 61, 188–203. https://doi.org/10.1016/j.ijpsycho.2005.10.001.

Lakatos, P., Karmos, G., Mehta, A.D., Ulbert, I., Schroeder, C.E., 2008. Entrainment of neuronal oscillations as a mechanism of attentional selection. Science 320, 110–113. https://doi.org/10.1126/science.1154735.

Lara, A.H., Wallis, J.D., 2015. The role of prefrontal cortex in working memory: a mini review. Front. Syst. Neurosci. 9, 173. https://doi.org/10.3389/fnsys.2015.00173.

Li, Z.H., Sun, X.W., Wang, Z.X., Zhang, X.C., Zhang, D.R., He, R., Hu, X.P., 2004. Behavioral and functional MRI study of attentional shift in human verbal working memory. Neuroimage 21, 181–191. https://doi.org/10.1016/j.neuroimage.2003.08.043.

Lobier, M., Siebenhühner, F., Palva, S., Palva, J.M., 2014. Phase transfer entropy: A novel phase-based measure for directed connectivity in networks coupled by oscillatory interactions. Neuroimage 85, 853–872. https://doi.org/10.1016/j.neuroimage.2013.08.056.

Lütkenhöner, B., Krumbholz, K., Seither-Preisler, A., 2003. Studies of tonotopy based on wave N100 of the auditory evoked field are problematic. Neuroimage 19, 935–949. https://doi.org/10.1016/S1053-8119(03)00172-1.

Matsubara, T., Ogata, K., Hironaga, N., Kikuchi, Y., Uehara, T., Chatani, H., Mitsudo, T., Shigeto, H., Tobimatsu, S., 2018. Altered neural synchronization to pure tone stimulation in patients with mesial temporal lobe epilepsy: An MEG study. Epilepsy Behav. 88, 96–105. https://doi.org/10.1016/j.yebeh.2018.08.036.

Mehnert, J., Bader, D., Nolte, G., May, A., 2019. Visual input drives increased occipital responsiveness and harmonized oscillations in multiple cortical areas in migraineurs. NeuroImage Clin. 23, 101815. https://doi.org/10.1016/j.nicl.2019.101815.

Min, B.K., Park, H.J., 2010. Task-related modulation of anterior theta and posterior alpha EEG reflects top-down preparation. BMC Neurosci. 11, 79. https://doi.org/10.1186/1471-2202-11-79.

Moore, A.B., Li, Z., Tyner, C.E., Hu, X., Crosson, B., 2013. Bilateral basal ganglia activity in verbal working memory. Brain Lang. 125, 316–323. https://doi.org/10.1016/j.bandl.2012.05.003.

Moretti, D.V., Babiloni, C., Binetti, G., Cassetta, E., Dal Forno, G., Ferreric, F., Ferri, R., Lanuzza, B., Miniussi, C., Nobili, F., Rodriguez, G., Salinari, S., Rossini, P.M., 2004. Individual analysis of EEG frequency and band power in mild Alzheimer's disease. Clin. Neurophysiol. 115, 299–308. https://doi.org/10.1016/S1388-2457(03)00345-6.

Naghavi, H.R., Nyberg, L., 2005. Common fronto-parietal activity in attention, memory, and consciousness: Shared demands on integration? Conscious. Cognit. 14, 390–425. https://doi.org/10.1016/j.concog.2004.10.003.

Ng, B.S.W., Logothetis, N.K., Kayser, C., 2013. EEG phase patterns reflect the selectivity of neural firing. Cerebr. Cortex 23, 389–398. https://doi.org/10.1093/cercor/bhs031.

Osaka, M., Osaka, N., Kondo, H., Morishita, M., Fukuyama, H., Aso, T., Shibasaki, H., 2003. The neural basis of individual differences in working memory capacity: an fMRI study. Neuroimage 18, 789–797. https://doi.org/10.1016/S1053-8119(02)00032-0.

Osaka, N., Osaka, M., Kondo, H., Morishita, M., Fukuyama, H., Shibasaki, H., 2004. The neural basis of executive function in working memory: an fMRI study based on individual differences. Neuroimage 21, 623–631. https://doi.org/10.1016/j.neuroimage.2003.09.069.

Payne, L., Kounios, J., 2009. Coherent oscillatory networks supporting short-term memory retention. Brain Res. 1247, 126–132. https://doi.org/10.1016/j.brainres.2008.09.095.

Postle, B.R., 2006. Working memory as an emergent property of the mind and brain. Neuroscience 139, 23–38. https://doi.org/10.1016/j.neuroscience.2005.06.005.

Razi, A., Seghier, M.L., Zhou, Y., McColgan, P., Zeidman, P., Park, H.J., Sporns, O., Rees, G., Friston, K.J., 2017. Large-scale DCMs for resting-state fMRI. Netw. Neurosci. 1, 222–241. https://doi.org/10.1162/NETN_a_00015.

Rodriguez Merzagora, A.C., Izzetoglu, M., Onaral, B., Schultheis, M.T., 2014. Verbal working memory impairments following traumatic brain injury: an fNIRS investigation. Brain Imaging Behav. 8, 446–459. https://doi.org/10.1007/s11682-013-9258-8.

Sakkalis, V., 2011. Review of advanced techniques for the estimation of brain connectivity measured with EEG/MEG. Comput. Biol. Med. 41, 1110–1117. https://doi.org/10.1016/j.compbiomed.2011.06.020.

Sarnthein, J., Petsche, H., Rappelsberger, P., Shaw, G.L., von Stein, A., 1998. Synchronization between prefrontal and posterior association cortex during human working memory. Proc. Natl. Acad. Sci. U. S. A. 95, 7092–7096. https://doi.org/10.1073/pnas.95.12.7092.

Sauseng, P., Klimesch, W., Doppelmayr, M., Hanslmayr, S., Schabus, M., Gruber, W.R., 2004. Theta coupling in the human electroencephalogram during a working memory task. Neurosci. Lett. 354, 123–126. https://doi.org/10.1016/j.neulet.2003.10.002.

Sauseng, P., Klimesch, W., Schabus, M., Doppelmayr, M., 2005. Fronto-parietal EEG coherence in theta and upper alpha reflect central executive functions of working memory. Int. J. Psychophysiol. 57, 97–103. https://doi.org/10.1016/j.ijpsycho.2005.03.018.

Sauseng, P., Klimesch, W., Freunberger, R., Pecherstorfer, T., Hanslmayr, S., Doppelmayr, M., 2006. Relevance of EEG alpha and theta oscillations during task switching. Exp. Brain Res. 170, 295–301. https://doi.org/10.1007/s00221-005-0211-y.

Sauseng, P., Klimesch, W., 2008. What does phase information of oscillatory brain activity tell us about cognitive processes? Neurosci. Biobehav. Rev. 32, 1001–1013. https://doi.org/10.1016/j.neubiorev.2008.03.014.

Schyns, P.G., Thut, G., Gross, J., 2011. Cracking the code of oscillatory activity. PLoS Biol. 9, e1001064. https://doi.org/10.1371/journal.pbio.1001064.

Seguin, C., Razi, A., Zalesky, A., 2019. Inferring neural signalling directionality from undirected structural connectomes. bioRxiv 573071. https://doi.org/10.1101/573071.

Serrien, D.J., Pogosyan, A.H., Brown, P., 2004. Influence of working memory on patterns of motor related cortico-cortical coupling. Exp. Brain Res. 155, 204–210. https://doi.org/10.1007/s00221-003-1720-1.

Sidtis, J.J., 1984. Music, pitch perception, and the mechanisms of cortical hearing. In: Gazzaniga, M.S. (Ed.), Handbook of Cognitive Neuroscience. Springer, Boston, MA. https://doi.org/10.1007/978-1-4899-2177-2_5.

Singer, W., 1999. Neuronal synchrony: a versatile code review for the definition of relations? Neuron 24, 49–65. https://doi.org/10.1016/S0896-6273(00)80821-1.

Thul, A., Lechinger, J., Donis, J., Michitsch, G., Pichler, G., Kochs, E.F., Jordan, D., Ilg, R., Schabus, M., 2016. EEG entropy measures indicate decrease of cortical information processing in Disorders of Consciousness. Clin. Neurophysiol. 127, 1419–1427. https://doi.org/10.1016/j.clinph.2015.07.039.

Varela, F., Lachaux, J.P., Rodriguez, E., Martinerie, J., 2001. The brainweb: Phase synchronization and large-scale integration. Nat. Rev. Neurosci. 2, 229–239. https://doi.org/10.1038/35067550.

Vartanian, O., Jobidon, M.-E., Bouak, F., Nakashima, A., Smith, I., Lam, Q., Cheung, B., 2013. Working memory training is associated with lower prefrontal cortex activation in a divergent thinking task. Neuroscience 236, 186–194. https://doi.org/10.1016/j.neuroscience.2012.12.060.

Weiss, S., Müller, H.M., Rappelsberger, P., 2000. Theta synchronisation predicts efficient memory encoding of concrete and abstract nouns. Neuroreport 11, 2357–2361. https://doi.org/10.1097/00001756-200008030-00005.

Westfall, P.H., Young, S.S., 1993. Resampling-based Multiple Testing: Examples and Methods for P-Value Adjustment. Wiley, New York.

Womelsdorf, T., Schoffelen, J.-M., Oostenveld, R., Singer, W., Desimone, R., Engel, A.K., Fries, P., 2007. Modulation of neuronal interactions through neuronal synchronization. Science 316, 1609–1612. https://doi.org/10.1126/science.1139597.

Yaoi, K., Osaka, M., Osaka, N., 2015. Neural correlates of the self-reference effect: evidence from evaluation and recognition processes. Front. Hum. Neurosci. 9, 383. https://doi.org/10.3389/fnhum.2015.00383.